A STUDY ON BUCKLING STRENGTH OF REINFORCED ANGLE STEEL POST IN TRANSMISSION TOWERS

Shunichi TAKAGI [1], Atsushi SATO [2]

SUMMARY

It has become a very important issue to establish a rational reinforcement method for transmission towers, since the increase of assumed loads resulting from revision of design standards. However, some methods have been established for replacing and reinforcing brace members, it's very difficult to replace the main post members.
In this study, we propose a reinforcement method in which reinforcement members are added to the existing main post angle members, and confirm the effectiveness of the reinforcement and its range of application by member compression tests.
The results showed that the reinforcement effect was sufficient when the slenderness ratio was large compared to the target reinforcement effect of this study. On the other hand, the reinforcement effect was not sufficient when the slenderness ratio was small.
In addition, from the examination of elastic buckling strength, the threshold of the region of flexural buckling and the region of lateral torsional buckling was examined, and it became clear that the buckling strength may be determined by lateral torsional buckling in the range of $\lambda c0 < 1.03$.

Keywords*: Transmission towers, Angle steel post, Flexural buckling strength, Torsional Buckling strength, Eccentric joint*

1. INTRODUCTION

In the case of transmission towers (hereinafter referred to as “Towers”), wind load is the predominant load due to its structural characteristics, and they are designed according to the Ministerial Ordinance (MO) [1)] for establishing technical standards. In recent years, there have been demands from society to increase the resilience of power distribution facilities, and in light of this, wind design methods [2)] that are in line with the actual conditions, including the introduction of regional wind speeds and gust response evaluations, have been reflected in the MO. Additionally, as towers designed to resist wind loads generally tend to have a reasonable seismic capacity, there has been a general tendency to omit seismic design. However, based on earthquake disaster experiences in recent years, there have been louder calls for the need to clarify seismic performance and implement seismic design, and seismic resistance standards for steel towers are being studied in light of this [3)]. With the increase in design load resulting from revisions to wind resistance/seismic design standards, existing towers may need to be retrofitted according to the results of the bearing capacity evaluation, and so establishing a rational method of tower reinforcement is clearly an important issue.

As shown in Fig.1, towers are generally comprised of a truss structure with four main members and diagonals that comprise the leg section and structural plane, respectively. There have been methods set for replacing and reinforcing members when repairing diagonal members, but due to the special construction methods required, replacing the main members is not a simple process. In this study, therefore, we examine a method of reinforcement that adds a new member to the angle steel post.

[1] *Graduate student, Graduate School of Engineering, Nagoya Institute of Technology, Japan, e-mail: cmn15010@nitech.jp*
[2] *Associate Professor, Graduate School of Engineering, Nagoya Institute of Technology, Japan, e-mail: sato.atsushi@nitech.ac.jp*

In regard to a reinforcement method for angle steel posts, Takatsuka et al. [4] conducted buckling tests in relation to a reinforcement method, in which existing members were sandwiched between the angle steel post members , and reported that buckling strength could not be increased when the slenderness ratio $\lambda \leq \lambda_c$, where λ_c is critical slenderness ratio . Arai et al and Fukuoka et al [5] conducted buckling tests using cross and overlay reinforcement methods, and reported the following results: for cross reinforcement, depending on the size of the reinforcement member, the buckling resistance is lower after reinforcement due to eccentric bending for test specimens with a slenderness ratio $\lambda = 40$, while overlay reinforcement decreases the buckling resistance, and joint slippage reduces the reinforcement effect. Ono et al. [6] conducted buckling tests using cross, fiber, and sandwich reinforcements and investigated these reinforcement effects; they found that the reinforcement increased bending stiffness. Komatsu et al. [7] performed buckling tests and numerical analysis for a reinforcement method using an assembly stiffener. Although some reinforcement effects were observed, they were limited with a small, normalized slenderness ratio range. Takamatsu et al. [8] confirmed and reported reinforcement effects using a carbon fiber plate with a monotonic compression and peak-to-peak alternating repetition tests.

These aforementioned studies were conducted on angle steel posts under ideal reinforcing conditions. However, for actual towers, a realistic reinforcement method is required because they comprise lap joint and diagonal members are attached to main members. Moreover, many studies only focused upon confirming the reinforcement effect. Evaluations of the reinforcement effect using dry bonding are limited to the study by Ono et al. [6], where the bending stiffness is multiplied by the experimental coefficients, and Komatsu et al. [7], where the evaluation is based on the moment of inertia, assuming a discrepancy between the existing and reinforcement membesr, and there have yet to be many quantitative evaluations.

Therefore, in this study,we examine the reinforcement effects of a reinforcement method aimed at angle steel posts in towers using member buckling tests. Considering the effect of bending eccentric joints and reinforcement, as well as the threshold of buckling behavior obtained from the elasticity theory solution, this study realizes potential application of the elasticity theory solution.

2. OVERVIEW OF THE REINFORCEMENT METHOD

Fig.2 demonstrates the reinforcement method employed in this study. As the angle steel posts in towers generally use the lap joints shown in Fig.1, eccentric bending is applied as a result of the eccentricity caused by the centers of the upper and lower members being misaligned. Studies suggesting the dangers of member-forced reduction due to this eccentric bending have been reported [9),10)] etc.. In response to this, this reinforcement method applies reinforcement members to the member to be reinforced, and adopts a structure in which the stress is transferred between the upper and lower existing members and the reinforcement through the splice plate (SPL), resulting in a structure similar to a butt-joint. This might reduce the structural eccentricity and improve cross-sectional performance.

In steel towers, angle steel posts are generally stacked alternatively on the inside and outside of the tower. In cases where the existing member to be reinforced is on the outside, the reinforcement member is attached on the inside and vice versa. Alternatively, if the member state in Fig. 2 is linear, the degree of additional bending is the same regardless of whether the member to be reinforced is inside or outside. As the direction of the additional bending does not affect the buckling force, our investigation shall focus on cases where the member to be reinforced is on the inside and the reinforcement member is on the outside.

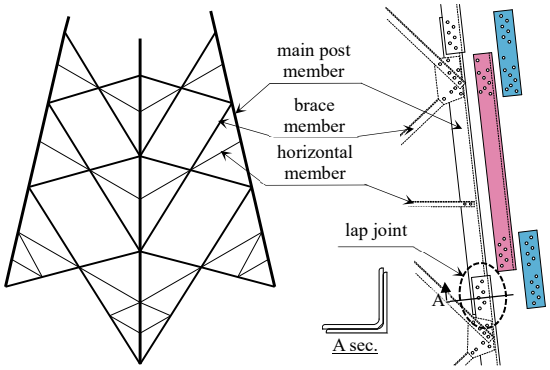

Fig.1 Overview of transmission towers

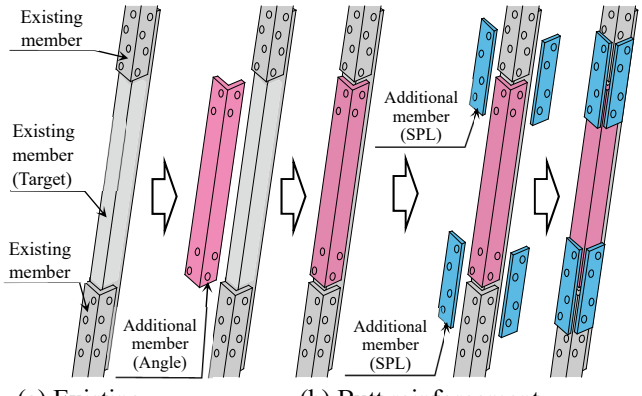

Fig.2 Reinforcement method

3. ANGLE STEEL POST BUCKLING TESTS

3.1 Overview of test specimens

We performed a compression test on the angle steel posts shown in section 2 to confirm the reinforcement effect. Table 1 shows the list of test specimens. The test parameters used were reinforcement size and slenderness ratio λ. We also set up a specimen that does not contain joints to confirm the effect of eccentric bending due to lap joints on the buckling resistance.

Here, λ : Slenderness ratio of existing member ($L/_{ex}r$) , ${}_{ex}r$: Existing member radius of gyration of area, λ_{c0} : Normalized slenderness ratio of existing members($\sqrt{N_Y/N_0}$), N_0 : Eulerian buckling load of existing member with member length as buckling length ($=\pi^2 E\cdot {}_{ex}I/L^2$), N_Y : Yield strength of existing members, ${}_{re}\lambda$: Slenderness ratio of reinforced material unit (${}_{re}L/{}_{re}r$), ${}_{re}r$: Reinforcement material radius of gyration of area.

Table 1 Test specimens and test result

No.	Existing member	Reinforcement method	Additional member	L (mm)	λ	${}_{c0}\lambda$	${}_{re}L$ (mm)	${}_{re}\lambda$	Remarks	${}_{com}\lambda_{c0}$	${}_{e}N_{cr}$ (kN)	$\frac{{}_{e}N_{cr}}{N_Y}$	γ
1	L150×10	No reinforcement	-	1188	40	0.61	-	-	No joint	0.61	1353.1	0.99	-
2				2376	80	1.22	-	-		1.22	833.8	0.61	-
3				3564	120	1.82	-	-		1.82	417.9	0.31	-
4				1188	40	0.61	-	-	Lap joint	0.61	853.5	0.62	-
5				2376	80	1.22	-	-		1.22	536.1	0.39	-
6				3564	120	1.82	-	-		1.82	333.0	0.24	-
7		Butt reinforcement using angle	L150×10	1188	40	0.61	158	5		0.59	1077.7	0.79	1.26
8				2376	80	1.22	1046	35		1.18	1224.2	0.89	2.28
9				3564	120	1.82	2234	75		1.77	724.0	0.53	2.17
10			L175×12	1188	40	0.61	158	5		0.54	1157.4	0.84	1.36
11				2376	80	1.22	1046	30		1.07	1345.1	0.98	2.51
12				3564	120	1.82	2234	65		1.61	910.0	0.66	2.73

L : Member length , λ : Slenderness ratio of existing member , λ_{c0} : Normalized slenderness ratio of existing member , ${}_{re}L$: Additional member length , ${}_{re}\lambda$: Slenderness ratio of additional mamber , ${}_{com}\lambda_{c0}$: Normalized slenderness ratio of combined cross section , ${}_{e}N_{cr}$: Buckling strength , N_Y : Yield strength , γ : Reinforcement ratio

Eqs.(1-5) express the performance of a section in which the existing member and reinforcement are assumed to be one single piece (hereinafter referred to as a combined cross-section).

$$ {}_{com}A = {}_{ex}A + {}_{re}A \tag{1} $$

$$ {}_{com}C_x = \frac{\left\{ {}_{ex}C_x \cdot {}_{ex}A + \left({}_{re}C_x + {}_{ex}t \right) \cdot {}_{re}A \right\}}{{}_{ex}A + {}_{re}A} \tag{2} $$

$$ {}_{com}I = {}_{ex}I + {}_{re}I + 2\left({}_{com}C_x - {}_{ex}C_x \right)^2 \cdot {}_{ex}A + 2\left({}_{re}C_x - {}_{re}t - {}_{com}C_x \right)^2 \cdot {}_{re}A \tag{3} $$

$$ {}_{com}r = \sqrt{{}_{com}I / {}_{com}A} \tag{4} $$

$$ {}_{com}\lambda_{c0} = 1/\pi \cdot \sqrt{\sigma_y / E} \cdot L / {}_{com}r \tag{5} $$

Here, ${}_{com}A$: Cross-sectional area of combined cross-section , ${}_{ex}A$: Cross-sectional area of existing member , ${}_{re}A$: Cross-sectional area of reinforcement member , ${}_{com}I$: Single specimen section moment of inertia of area, ${}_{ex}I$: Single specimen section moment of inertia of existing member , ${}_{re}I$: Single specimen section moment of inertia of reinforcement material , ${}_{com}r$: Single specimen section radius of gyration of area , ${}_{com}\lambda_{c0}$: Normalized slenderness ratio of combined cross-section , E : Young's modulus , with the definition of other symbols as shown in Fig.3.

For a slenderness ratio λ of 40, 80, or 120, including the inelastic buckling region, the size of the reinforcement member should be the same size as the existing member or one size larger.

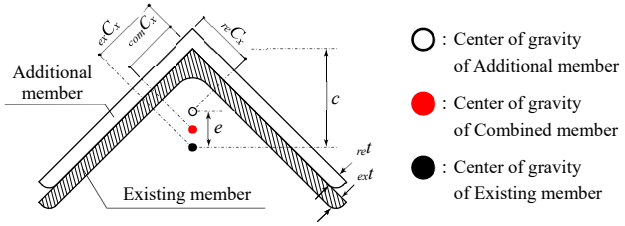

Fig.3 Symbols

Fig.4 illustrates examples of the test specimen shapes. As common items used for test specimens (No.4-12) with joints, ten M24 joint bolts with a joint length of 400 mm were used, with the bolt arrangement was the same. The

bolt strength region, in accordance with conventional towers, was set to 9.8 (hot dip galvanized bolts). The bolts are tightened following standard procedures for towers; after applying rapeseed oil to the bolts, they were tightened to a tightening torque of 430 N-m.

The number of reinforcement member mounting bolts are basically the same as the joint bolts; however, for No.7 and No.10 test specimens, where there is little space between the joints, dimensionally speaking, a maximum of four bolts can be accommodated.

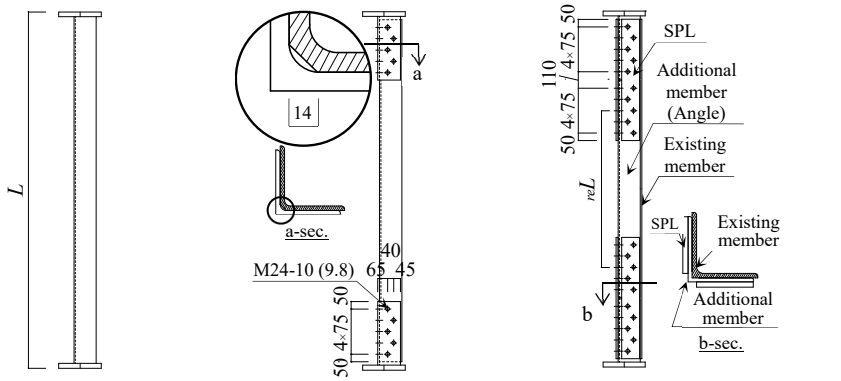

(a) No joint (b) With joint (c) Reinforcing angle member

Fig.4 Test specimens (unit:mm)

All materials simulate those used in actual tower, with the angular steel used being the L150×10 (SS540) and L175×12 (SS540) types conventionally used for towers, and thick plates of 12mm (SM490) used for the SPL. Surface treatment is not performed on the lap joints section or reinforcement section.

Table 2 shows the mechanical properties of the steel materials after hot dip galvanizing with the JIS Z 2241 1A test piece, whereas Table 3 shows the combined cross-section performance of the existing members and reinforcement members. The radius of gyration of area increase ratio ${}_{com}r$ /${}_{ex}r$, in case of the same size reinforcement is 3%, and in case of reinforcements one size larger, this is 10%.

Table 2 Material properties from tensile test

Member	Material	E (N/mm^2)	σ_y (N/mm^2)	σ_u (N/mm^2)	$Y.R.$ (%)
L150×10	SS540	216000	469	613	76.5
L175×12		221000	425	576	73.8
SPL-12	SM490	212000	361	492	73.4

Table 3 Section properties

Member		${}_{com}A$ / ${}_{ex}A$	${}_{com}I$ / ${}_{ex}I$	${}_{com}r$ / ${}_{ex}r$
Existing	Additional			
L150×10	-	1.00	1.00	1.00
L150×10	L150×10	2.00	2.11	1.03
L150×10	L175×12	2.39	2.90	1.10

3.2 Measurement and loading overview

Fig.5 shows a loading overview diagram, displacement, and strain measurement locations. Vertical displacement meters include those installed at two locations between the pin jig fulcrums, stress on all members is calculated using the attached strain gauges as shown in the Fig.5.

The loading used shall be monotonic compression loading using an Amsler-type long-column testing device. In the testing device used in this experiment, the center of rotation of the pin jig installed at the upper and lower ends of the testing machine is aligned with the contact surface for the test piece [6]. For this reason, the total length of the specimen, including the thickness of the end plate, equates to the buckling length (lumber length L). Additionally, the planar center of rotation is aligned with the upper and lower existing member centers of gravity. The load is measured with a load cell installed in the testing device.

3.3 Testing results

The relationship between load and axial deformation is shown in Fig.6, and the test results are shown in Table 1. The vertical axis in Fig.6 and vertical axis in Fig.7 show the nondimensional value of the load N in terms of the yield strength of the existing member, N_Y, and load N in terms of the yield strength of the existing member, N_Y, respectively. In terms of the horizontal axis, the vertical displacement δ between the pin jig supports is a nondimensional value of elastic deformation δ_y ($=N_Y \cdot L/(E \cdot {}_{ex}A)$) in relation to the yield capacity.

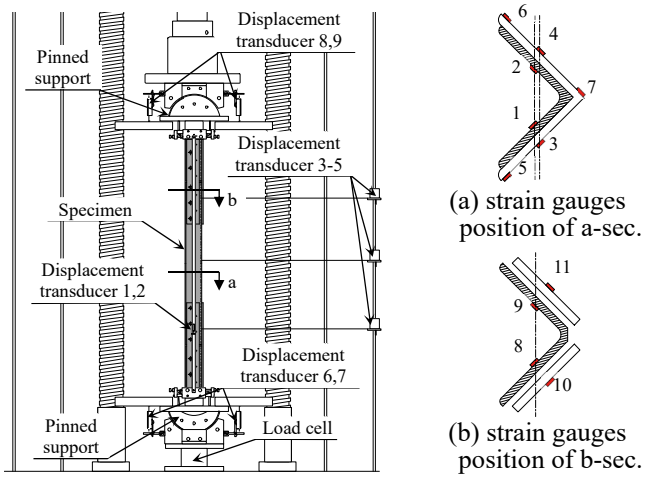

Fig.5 Test setup and strain gauges position

From Fig.6, we could confirm that in test specimens of $\lambda \leqq 80$, joint slippage behavior. On the other hand, test specimens at λ=120 did not exhibit clear sliding behavior. As shown in Fig.7, a jointless test piece (No.1) λ=40 demonstrates maximum bearing capacity due to torsional buckling. However, this is followed by rapid degradation of bearing capacity. However, as there was no displacement measurement after the point of bearing capacity deterioration, Fig.6 represents the maximum bearing capacity. For other test specimens, the maximum bearing capacity was developed by bending buckling in which the center of the member was at the maximum deformation position, and this indicates a gradual degradation in bearing capacity.

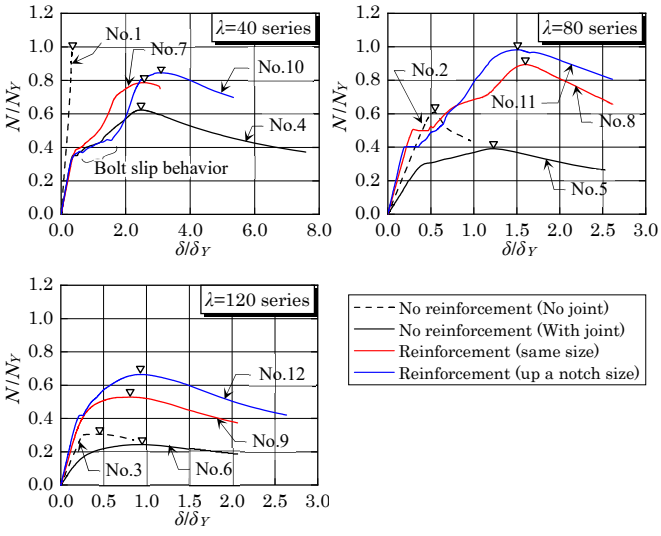

Fig.6 $N/N_Y - \delta/\delta_Y$ relation

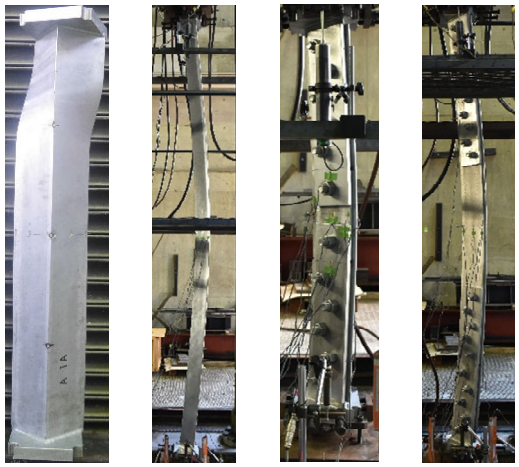

Fig.7 Deformation after loading

Buckling strength (hereinafter "AIJ buckling strength") curves and test results based on the Allowable Stress Design of Steel Structures [11], in addition to the results of a buckling strength evaluation based on the normalized slenderness ratio λ_{c0}, are shown in Fig.8. The AIJ buckling strength is calculated by deducting the safety factor ν from the short-term load buckling resistance.

If we compare nonreinforced test specimens based on whether they have a joint, as λ_{c0} increases, the difference in buckling strength depending on the existence of a joint increases.

If uniform bending is applied to a member on which load N is applied in a position with eccentricity e in the same direction, the horizontal elastic deflection δ at the center of the member considering geometric nonlinearities is approximated by Eq.(6). Additionally, the maximum bending moment that occurs in the center of the member considering geometric nonlinearity can be expressed as Eq.(7).

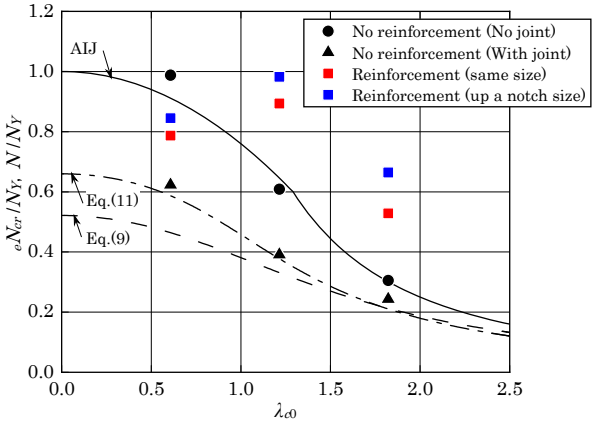

Fig.8 $N/N_Y - \lambda_{c0}$ relation

$$\delta = e\left(\sec\frac{\pi}{2}\sqrt{\frac{N}{N_0}} - 1\right) \quad (6), \qquad M = N(\delta + e) = N \cdot e \cdot \sec\frac{\pi}{2}\sqrt{\frac{N}{N_0}} \quad (7)$$

The following equation expresses the edge stress intensity σc at elasticity of a member subjected to an eccentric compressive force.

$$\sigma_c = N/A + M/Z \quad (8)$$

The point at which the edge stress intensity reaches the yield stress level, under design guidelines for steel structure buckling [12] is used as a way of evaluating buckling resistance, and in such a case, for the buckling resistance formula, $\sigma_c = \sigma_y$ and Eq.(7) are substituted in Eq.(8), and the following equation can be derived using the Taylor expansion.

$$\frac{N}{N_Y} = \frac{\left\{1+\frac{8}{\pi^2}\left(1+\frac{e\cdot A}{Z}\right)\cdot\frac{1}{\lambda_{c0}{}^2}\right\} - \sqrt{\left\{1+\frac{8}{\pi^2}\left(1+\frac{e\cdot A}{Z}\right)\cdot\frac{1}{\lambda_{c0}{}^2}\right\}^2 - \frac{32}{\pi^2}\cdot\frac{1}{\lambda_{c0}{}^2}}}{2} \quad (9)$$

Here, e : eccentric distance due to the joint, A : cross-sectional area, Z : cross-section coefficient.

Fig.8 shows the buckling strength curve due to Eq.(9) as a broken line. Eq.(9) underestimates the experiment results. On the other hand, in the case of the center of members where additional bending moment is at a maximum, no localized bending occurs, and unstable phenomena did not occur. Additionally, based on the *M*-*N* correlation diagram obtained from the experiment results shown in Fig.9, the load N satisfying Eq.(10) reaching the fully-plastic state at the time of buckling, the buckling resistance N_{cr} can be derived by substituting Eq.(7) into Eq.(10) and using Taylor expansion, as in Eq.(11). M and N in the experiment results in Fig.9 indicate the values obtained from the strain values of the center cross-sections of the members.

$$\frac{N}{N_Y} + \frac{M}{M_p} = 1 \quad (10), \qquad \frac{N}{N_Y} = \frac{\left\{1+\frac{8}{\pi^2}\left(1+\frac{e\cdot A}{Z_p}\right)\cdot\frac{1}{\lambda_{c0}{}^2}\right\} - \sqrt{\left\{1+\frac{8}{\pi^2}\left(1+\frac{e\cdot A}{Z_p}\right)\cdot\frac{1}{\lambda_{c0}{}^2}\right\}^2 - \frac{32}{\pi^2}\cdot\frac{1}{\lambda_{c0}{}^2}}}{2} \quad (11)$$

The dotted line in Fig.8 indicates the buckling strength curve resulting from Eq.(11). From the same figure, we can see that there is good correspondence between the buckling resistance $_eN_{cr}$ and Eq.(11) of the nonreinforced test specimens with joints within the scope of this experiment, and the reduction in bearing capacity due to eccentric joints can be competently evaluated using the buckling resistance N_{cr} as N in Eq.(11) based on the full plasticity correlation equation.

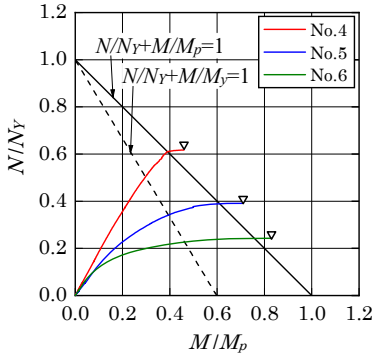

Fig.9 $M - N$ interrelation

If we compare the difference in reinforcement material size for the reinforcement test specimens, the buckling resistance of the specimen reinforced with one size larger was greater than the specimen reinforced with the same size as the existing specimen, regardless of the slenderness ratio.
With $\lambda_{c0} \geq 1.22$, using this reinforcement method, it could be confirmed that the buckling resistance and AIJ buckling strength of the nonreinforced specimens without joints was exceeded. However, in the case of λ_{c0} =0.61, the buckling resistance and AIJ buckling strength was lower than the nonreinforced specimens without joints. Furthermore, the buckling resistance after reinforcement in case of λ_{c0} =0.61 was smaller than the buckling resistance after reinforcement of λ_{c0} =1.22, and a factor in this is thought to be the effect of the missing bolt holes that exist only in the specimens with λ_{c0} =0.61 (No.7 and 10) near the center section of the member, where the stress intensity is the most severe.

3.4 Reinforcement effect

When considering whether to apply reinforcement to actual towers, if the allowable stress ratio (= considered stress intensity/allowable stress) of a certain main member is extremely high, it can be assumed that there is a wide range of under-strength members, and there is a high possibility that reinforcement would not be applied. Therefore, in consideration of workability and economy, the target value in this study satisfies the allowable stress ratio of 1.0 to 1.3 by reinforcement. That is to say, reinforcement γ >1.3.
Fig.10 shows the reinforcement effect γ obtained in this test. γ is the buckling resistance ${}_eN_{cr}$ of the reinforced specimen divided by the buckling resistance ${}_eN_{cr}$ of the nonreinforced specimen with joints. With λ_{c0} =0.61, γ = 1.26－1.36, but at $\lambda_{c0} \geq 1.22$, γ > 2.0, and a sufficient reinforcement effect is obtained.

Fig.11 shows the relationship between the normalized slenderness ratio λ_{c0} of ${}_eN_{cr}$ / ${}_{com}N_Y$ as the existing member unit and the normalized slenderness ratio ${}_{com}\lambda_{c0}$ of the combined cross-section. Regardless of λ_{c0}, ${}_{com}\lambda_{c0}$, the nondimensional buckling strength with ${}_{com}N_Y$ was below the AIJ buckling strength. With this reinforcement, although a reduction in eccentric bending can be expected by attaching the reinforcement materials and SPL, as this is below the AIJ buckling strength, the impact of the eccentric bending can be expected to remain, and it is important to appropriately evaluate eccentricity in this reinforcement method. On the other hand, the tendency of the λ_{c0} = 0.61 test specimen is greatly changed.

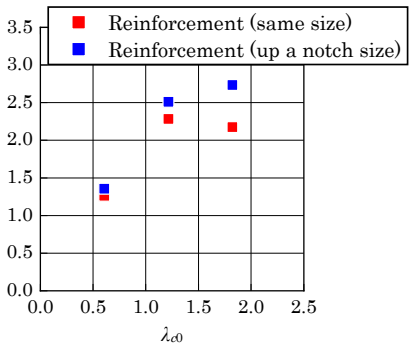

Fig.10 Reinforcement ratio－λ_c relation

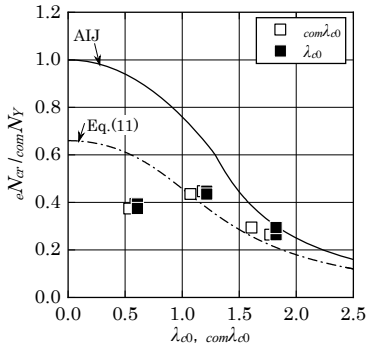

Fig.11 $N/{}_{com}N_Y$ －λ_{c0} , ${}_{com}\lambda_{c0}$ relation

4. ELASTIC BUCKLING RESISTANCE OF UNIAXIALLY SYMMETRICAL SECTION MEMBERS SUBJECTED TO COMPRESSIVE AXIAL FORCE

From the results in section 3, we can hypothesize that the mechanism by which this reinforcement method contributes to the buckling resistance after reinforcement differs according to slenderness ratio λ, and the main cause is considered to be the discrepancy in buckling behavior. In the Allowable Stress Design of Steel Structure [11)], it states that if the plate elements are sufficiently small and localized buckling is not a concern, the bearing capacity is determined by bending buckling, and so the predominant buckling mode is bending buckling (total buckling). Based on this, the normalized slenderness ratio λ_{c0} is generally defined as $\sqrt{N_Y/\min(P_x,P_y)}$ based on the elastic buckling resistance of the predominant buckling mode (buckling resistance P_x , P_y around each axis) and yield strength N_Y. As in the case of open cross-sections such as angular steel posts, it is necessary to consider flexural torsional buckling, it becomes necessary to investigate elastic buckling strength P_e, to be described later. Further, for angular steel posts in areas with a small slenderness ratio, due to the predominance of elastic flexural torsional buckling, this reinforcement method, which is expected to have a reinforcing effect by increasing the bending stiffness, is not considered to be sufficiently effective as it gets closer to the region. Therefore, in this

section, a wire-based elastic buckling theory is used to examine the threshold of buckling behavior.

In the center of the figure, we studied the elastic buckling resistance of uniaxially symmetrical cross-sectional members subjected to compressive axial force. Fig.12 (a) and (b) show the form of the member cross section and the boundary conditions for the material end, respectively. Here, *O* in the member cross-section is the shear center. If torsion occurs in the cross-section, the shear center becomes the center of rotation.

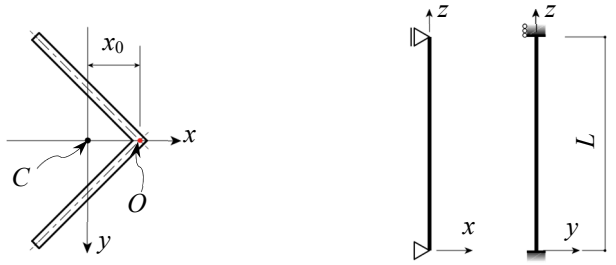

(a) Cross sectional shape (b) Boundary conditions

Fig.12 Cross section and Boundary conditions

The elastic buckling resistance P_{cr} of the member receiving compression axial force can be derived from the force balance at the point of infinitesimal deformation at the moment of buckling. The force balancing equation is obtained as follows [13] by expressing the displacements in the x and y directions at the moment of buckling as u and v, and the torsional angle of the cross section as β.

$$EI_y \frac{d^2u}{dz^2} = -P \cdot u \qquad (12), \qquad EI_x \frac{d^2v}{dz^2} = -P\left(v - x_0 \cdot \beta\right) + EI_x \left(\frac{d^2v}{dz^2}\right)_{z=0} \qquad (13)$$

$$EI_w \frac{d^4\beta}{dz^4} - \left(GJ - \frac{I_0}{A}P\right)\frac{d^2\beta}{dz^2} - P \cdot x_0 \frac{d^2v}{dz^2} = 0 \qquad (14)$$

As Eq.(12) does not include the cross-section angle of torsion β, elastic buckling occurs in the plane (x-z plane) including the axis of symmetry in the cross-section, and the elastic flexural buckling strength, P_y, corresponds to the Eulerian buckling resistance, P_E.

$$P_y = \frac{\pi^2 EI_y}{L^2} \qquad (15)$$

Based on Eqs.(13),(14) and the member end boundary conditions, the following equation can be obtained as a formula for calculating critical load.

$$\begin{vmatrix} P - P_x & -P \cdot x_0 \\ -P \cdot x_0 & \frac{I_0}{A}\left(P - P_\beta\right) \end{vmatrix} = 0 \qquad (16)$$

Here, P_x, P_β are values expressed in the following equation, and correspond to elastic flexural buckling strength around the x-axis and elastic torsional buckling strength around the z-axis.

$$P_x = \frac{\left(2\pi\right)^2 EI_x}{L^2} \qquad (17), \qquad P_\beta = \frac{A}{I_0}\left\{GJ + EI_w\left(\frac{2\pi}{L}\right)^2\right\} \qquad (18)$$

As a result, Eq.(19) is obtained and its root is elastic buckling resistance P_{cr}.

$$\frac{I_c}{I_0}P^2 - \left(P_x + P_\beta\right)P + P_x \cdot P_\beta = 0 \qquad (19), \qquad P_{cr} = \frac{\left(P_x + P_\beta\right) \pm \sqrt{\left(P_x + P_\beta\right)^2 - 4\left(I_c/I_0\right)P_x \cdot P_\beta}}{2\left(I_c/I_0\right)} \qquad (20)$$

Here, I_c and I_0 are the polar moment of inertia around the center of the figure, and the polar moment of inertia around the sheer center, respectively, and are expressed in the following equations.

$$I_c = I_x + I_y \qquad (21), \qquad I_0 = I_x + I_y + A\left(x_0\right)^2 = I_c + A\left(x_0\right)^2 \qquad (22)$$

Eq.(20) provides two solutions for the elastic buckling resistance P_{cr}, and the relationship between the two elastic buckling resistances P_{cr} and the elastic flexural buckling strength P_x around the x-axis, and the elastic torsional buckling strength P_β around the z-axis is shown in Fig.13. The value of I_0/I_c is ~1.6 for isosceles angular steel posts.

Here, the small root of Eq.(20) or the Eulerian buckling resistance in the plane of symmetry is the elastic buckling resistance, and this is expressed by the following equation.

$$P_e = \min\left\{P_y, P_{cr}\right\} \qquad (23)$$

A comparison of the various elastic buckling resistances for the angular steel post sizes (L150×10) on which the buckling tests were performed is shown in Fig.14. Furthermore, as in the actual towers the restraint conditions on the end sections are the same in both the x and y directions, the buckling length is L when calculating P_x.
From Fig.14 , we can see that for L150×10, $P_y < P_{cr}$ when $\lambda_{c0} > 1.03$, and the predominant elastic buckling behavior is bending buckling around the weak axis. So we can see that in case of $\lambda_{c0} < 1.03$, $P_{cr} < P_y$, and the predominant elastic buckling behavior is to be impacted by flexural-torsional buckling.

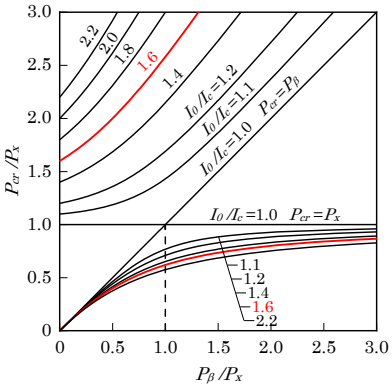

Fig.13 Relationship between elastic buckling Strength and cross sectional shape

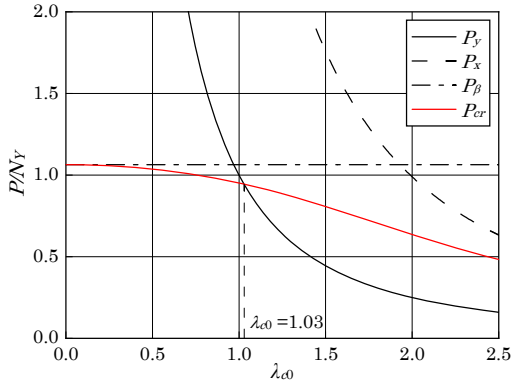

Fig.14 Elastic buckling Strength for L150×10

5. CALCULATING RESISTANCE AFTER REINFORCEMENT

The results of this study can only be applied to the L150×10 members and joints of the same size as those used in Section 3. In terms of the structures to be reinforced in this study, it is necessary to consider both the increase in cross-sectional performance due to reinforcement and the effect of eccentric bending due to joints. For this reason, the post-reinforcement resistance in this study is considered separately for both elements, and the buckling resistance, which takes into account the improvement in cross-sectional performance due to reinforcement , is multiplied by a reduction factor for bearing capacity due to bending of the eccentric joints.

If the ratio of the AIJ buckling strength and Eq.(11) shown in Fig.8 is taken as the bearing capacity reduction factor α due to eccentric bending, the relationship is as shown in Fig.15. Next, the AIJ buckling strength is expressed by the following equation, excluding the safety factor ν.

In case of $\lambda \leqq \Lambda$

$$N_{AIJ} = \left\{1 - 0.4\left(\frac{\lambda}{\Lambda}\right)^2\right\}\sigma_y \cdot A \qquad (24.a)\ ,$$

In case of $\lambda > \Lambda$

$$N_{AIJ} = \frac{\pi^2 E}{\lambda^2} \cdot A \qquad (24.b)$$

λ is the slenderness ratio on a ${}_{com}\lambda$, A is the cross-section area on an ${}_{com}A$, ${}_{com}N_{AIJ}$ on a combined cross-section can be obtained. Additionally, by seeking the buckling strength ${}_{ex}N_{AIJ}$, ${}_{re}N_{AIJ}$ for the existing member and reinforcement member respectively, the buckling resistance when they are combined can be obtained.

The reduction coefficient α and calculation formula ${}_cN_{cr}$ for bearing capacity after reinforcement based on Eq.(24) are expressed as follows.

$${}_cN_{cr} = \alpha \cdot {}_{com}N_{AIJ} \quad \text{(combined cross-section)} \quad (25)\ , \qquad {}_cN_{cr} = \alpha \cdot \left({}_{ex}N_{AIJ} + {}_{re}N_{AIJ}\right) \quad \text{(superposition)} \quad (26)$$

Fig.16 shows the relationship between ${}_eN_{cr}$ / ${}_cN_{cr}$ and the λ_{c0}. In the case of $\lambda_{c0} > 1.03$, reinforcement test specimens ${}_cN_{cr}$ are slightly underestimated in both Eqs.(25) and (26) and an evaluation is given on the safety side. On the other hand, in the case of $\lambda_{c0} < 1.03$, nonreinforcement test specimens ${}_cN_{cr}$ provide a good estimate for experimental results, but overestimate for reinforcement test specimens, and do not provide an adequate evaluation of the reinforcement effect in the region of predominant flexural-torsional buckling.

No significant difference in the post-reinforcement capacity was observed between cases in which the reinforcement members were assumed to be a single section and those in which the existing members and the reinforcing members overlapped each other. In addition, the inappropriate evaluation of bearing capacity in the slender ratio region where flexural-torsional buckling is assumed to be predominant, and the extension of the reduction factor α to arbitrary member sizes are also future issues.

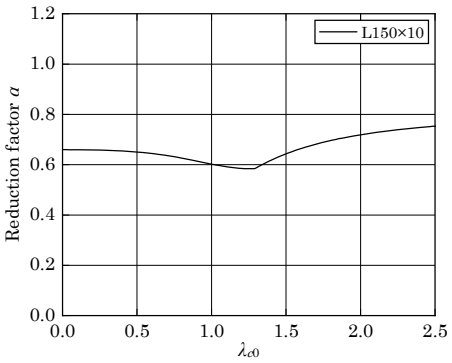

Fig.15 Reduction factor α

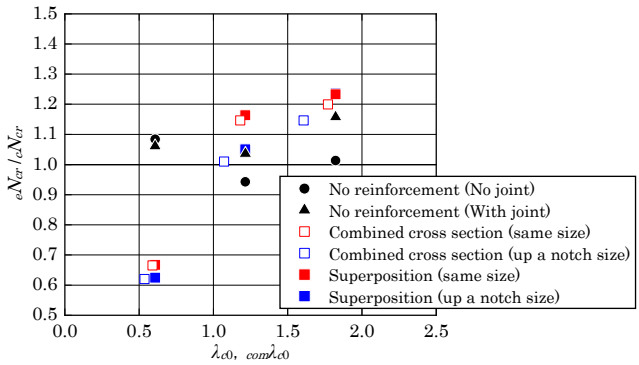

Fig.16 $_{e}N_{cr}$ / $_{c}N_{cr}$ − $\lambda_{c0,com}\lambda_{c0}$ relation

6. SUMMARY

In this paper, we conducted buckling tests on angle steel posts that were the main members of angular steel towers for transmission. the results of which are shown below.

1) Eq.11, which is based on the full plasticity correlation equation, can be used to provide a good evaluation of the reduction in bearing capacity due to eccentric bending caused by the existence of joints.
2) In regard to the target reinforcement effects in this study, in relation to $\gamma > 1.3$, in $\lambda_{c0} \geq 1.22$, the reinforcement effect is $\gamma > 2.0$ and an appropriate reinforcement effect could be confirmed. On the other hand, with $\lambda_{c0} = 0.61$, this stopped at $\gamma = 1.26 - 1.36$, and a sufficient reinforcement effect could not be obtained.
3) We examined the threshold of the region of predominant flexural buckling and the region of predominant flexural-torsional buckling based on a theoretical solution of elastic buckling resistance, and it was found that $\lambda_c = 1.03$ is the bifurcation point of buckling behavior for L150×10, which is the subject of this paper.
4) The resistance after reinforcement cNcr in the region where bending buckling is predominant was evaluated to be on the safe side by multiplying the buckling load capacity of the assumed combined cross-section and the overlap of the existing member, as well as the reinforced material by resistance reduction factor α due to the bending of the eccentric joints.

REFERENCES

1) METI：Ministry Ordinance that sets Technical Standards for Electrical Equipment (in Japanese)
2) IEEJ：Design standards on structures for transmission JEC-TR-00007-2015,2015 (in Japanese)
3) ETRA：Seismic Design of Transmission Towers and Issues,Vol.73,No.3,2018 (in Japanese)
4) Takatsuka, S.,Miyauchi, Y.,Ishii, Y.,Ogata, M.：Reinforcement of existing angle steel truss member,Summaries of technical papers of annual meeting,AIJ,pp.1147-1148,1994 (in Japanese)
5) Arai, S.,Hongo, E.,Mikami, Y.,et al.：Study on buckling strength of cross section members for steel tower,Summaries of technical papers of annual meeting,AIJ,pp.507-508,2001 (in Japanese)
6) Kozawa, H.,Ono, T.,Ishida, K.,et al.：Experiment of the reinforced angle members for buckling on truss tower,Summaries of technical papers of annual meeting,AIJ,pp.829-830,2006 (in Japanese)
7) Numayama, N.,Komatsu, H.,Ishii, K. ,Yagi, S.：Study on buckling strength of angle steel compression members reinforced by the built-up method Part.5 Evaluation of buckling strength,Summaries of technical papers of annual meeting,AIJ,pp.955-956,2013 (in Japanese)
8) Hattori, A.,Tamai, H.,Yamanishi, T.,et al.：Design formula for rehabilitated angle steel member using carbon fiber reinforced plastic plates,Journal of structural and construction engineering (Transactions of AIJ),No.659,pp.175-183,2011 (in Japanese)
9) Sato, A.,Mitsui, K.,Ono, T.：Flexural buckling stregth of steel angle member with eccentric joint,Journal of structural and construction engineering (Transactions of AIJ),No.726,pp.1343-1353,2016 (in Japanese)
10) Nakamura, T.,Ishida, T.,Igawa, N.：A study on buckling strength of angle member with lap joint in the existing truss steel tower for power transmission,Steel construction engineering (Transactions of JSSC),vol.27,No.108,pp.83-91,2020 (in Japanese)
11) AIJ：Allowable Stress Design of Steel Structures,2019 (in Japanese)
12) AIJ：Recommendations for Stability Design of Steel Structures,2018 (in Japanese)
13) Stephen P. Timoshenko,James M. Gere：THEORY OF ERASTIC STABILITY,1961